Supporting Information for

Monodisperse $Na_xY(OH)_yF_{3+x-y}$ Mesocrystals with Tunable Morphology and Chemical Composition: pH-Mediated Ion-Exchange

Jiao Wang,*,†,# Bi-Qiu Liu,‡,# Gaoshan Huang,§,// Zhi-Jun Zhang,*,⊥ and Jing-Tai Zhao⊥

†School of Information Science & Engineering and §Department of Materials Science, Fudan University, Shanghai 200433, P. R. China

‡Shanghai Institute of Ceramics, Chinese Academy of Sciences, Shanghai, 200050, P. R. China

// National Key Laboratory of Fundamental Science of Micro/Nano-Device and System Technology, Chongqing University, Chongqing 400030, P. R. China

⊥School of Materials Science and Engineering, Shanghai University, Shanghai, 200072, P. R. China

Chemical Composition and Crystal Structure.

The crystal structures of powder samples were refined from XRD data using FullProf software package,[1] and the crystal structure of $Y(OH)_{1.57}F_{1.43}$ was taken as original structural model. Morphology and particle size were observed by a scanning electron microscopy (SEM, S-4800) and transmission electron microscopy (TEM, JEOL200CX). Infrared spectra were obtained by the KBr pellet method on a Fourier Transform infrared (FTIR) spectrophotometer (Nicolet Avatar 370). The chemical compositionwas confirmed using powdered sample by inductibely coupled plasma-optical emission spectroscopy (ICP-OES) on a BarianVista RL spectrometer with radial plasma obserbation.

Table S1. The chemical composition of as-prepared samples obtained under the different pH values conditions measured by ICP-OES spectrometry.

pH value	$Na_xY(OH)_yF_{3+x-y}$	sample
12.0	$Na_{0.863(2)}Y_{1.00(2)}O_{0.62(3)}H_{0.40(2)}F_{3.4(2)}$	S1
12.3	$Na_{0.524(5)}Y_{1.000(8)}O_{1.23(1)}H_{1.17(6)}F_{2.45(2)}$	S2
12.4	$Na_{0.309(6)}Y_{1.000(5)}O_{1.68(1)}H_{1.71(2)}F_{1.801(6)}$	S3
12.6	$Na_{0.274(2)}Y_{1.000(5)}O_{1.55(3)}H_{1.76(2)}F_{1.698(2)}$	S4
12.7	$Na_{0.201(2)}Y_{1.000(4)}O_{1.76(7)}H_{1.88(3)}F_{1.46(4)}$	S5
12.9	$Na_{0.180(3)}Y_{1.000(2)}O_{2.03(7)}H_{2.02(3)}F_{1.36(2)}$	S6
13.1	$Na_{0.156(1)}Y_{1.000(6)}O_{2.47(7)}H_{2.12(3)}F_{1.23(2)}$	S7
13.3	$Na_{0.140(2)}Y_{1.000(7)}O_{2.29(6)}H_{2.13(3)}F_{1.195(8)}$	S8
13.4	$Na_{0.117(5)}Y_{1.000(2)}O_{3.06(9)}H_{2.5(2)}F_{0.898(8)}$	S9
13.5	$Na_{0.090(2)}Y_{1.000(2)}O_{2.757(2)}H_{2.56(2)}F_{0.835(4)}$	S10
13.6	$Na_{0.1008(4)}Y_{1.000(3)}O_{2.92(4)}H_{2.59(8)}F_{0.660(4)}$	S11
13.7	$Na_{0.068(2)}Y_{1.000(1)}O_{2.92(7)}H_{2.72(3)}F_{0.544(5)}$	S12
13.8	$Na_{0.051(3)}Y_{1.000(2)}O_{2.85(6)}H_{2.73(13)}F_{0.470(2)}$	S13

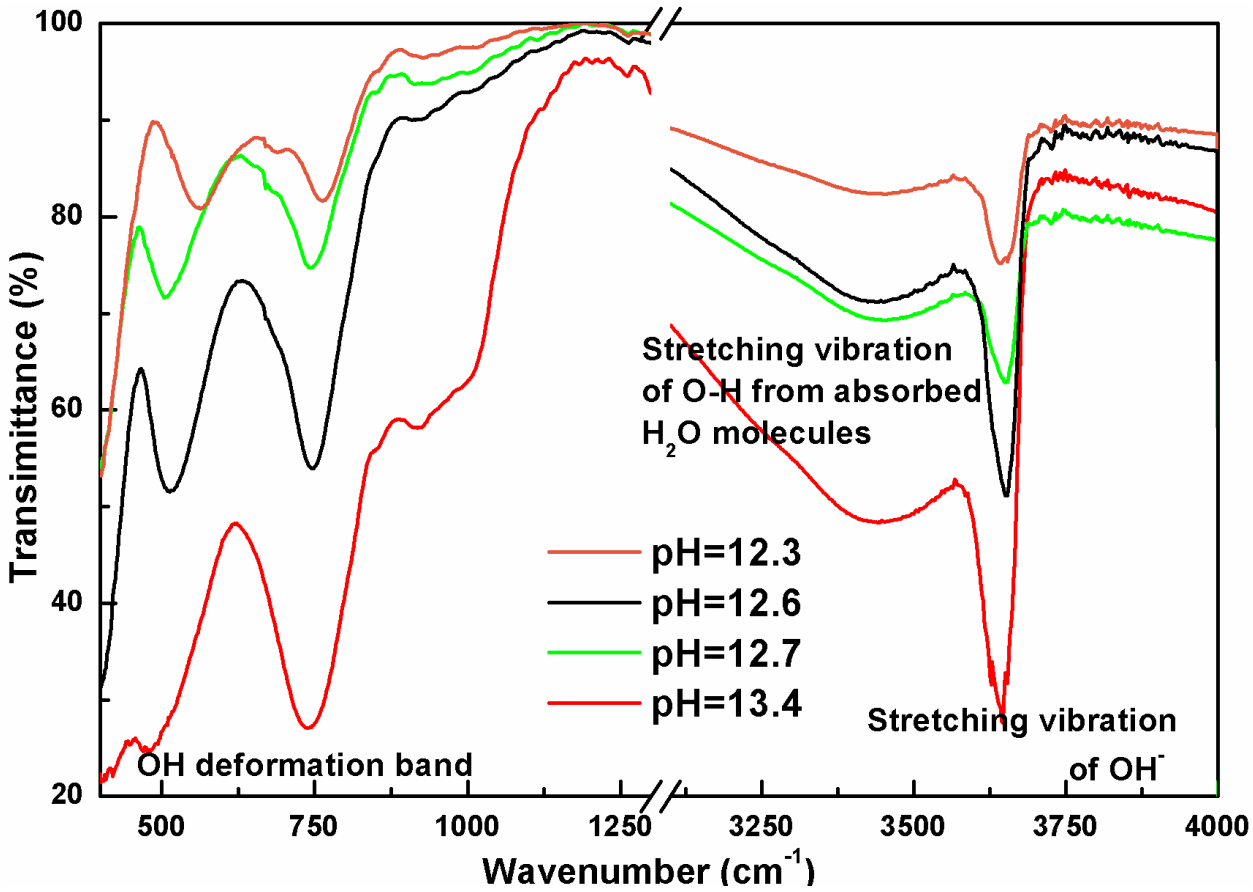

Figure S1. FT-IR spectra of samples obtained in the initial solutions with different pH values (the wavenumber differences of absorption band due to OH deformation vibration modes are marked).

The broad band around 3400 cm^{-1} is assigned to the stretching and bending of O-H vibrations in water in the air or adsorbed on the surface of the sample. The FTIR spectra confirm the fact that the as-prepared sample contains OH^- group due to the presence of the OH^- deformation bands around 500 cm^{-1} and 750 cm^{-1} as well as intense and sharp peak around 3600 cm^{-1} (Figure S1). The OH^- deformation bands shifting towards lower frequencies is believed to be related to the enhanced hydrogen bonding between the OH groups and F atom. [2, 3] The deformation bands surely shift to lower frequencies with decreasing fluorine contents (Figure S1). In the other hand,

the sharpness of the OH^- stretching vibration of absorption gives support that there is presumably little or no hydrogen bonding in $Y(OH)_3$, [4-6] since hydrogen bonding tends to lower and broaden the OH stretching frequency. The sharpness is apparently increased with decreasing fluorine contents in $Na_xY(OH)_yF_{3+x-y}$, which is considered to contain mostly hydrogen bonds. [6]

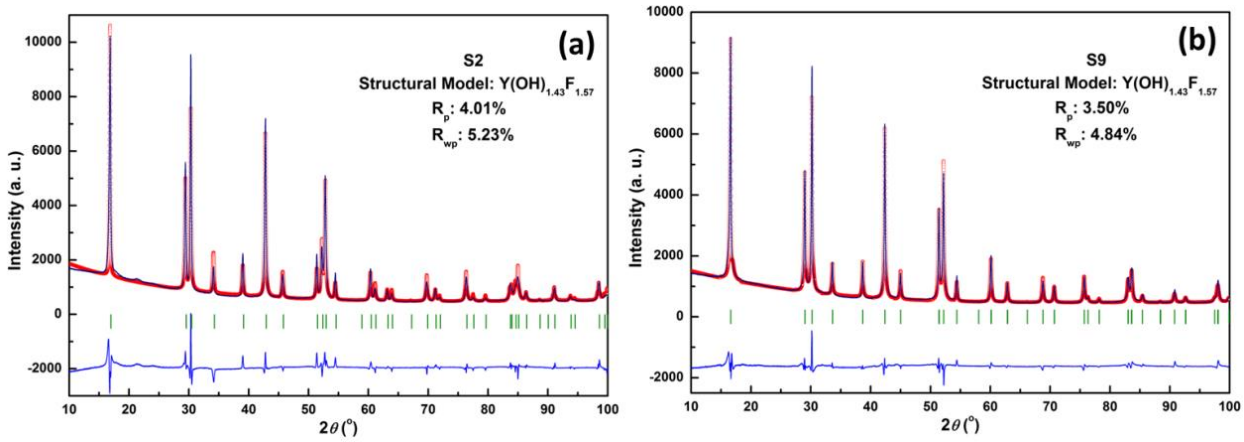

Figure S2. The Rietveld refinements of powder XRD patterns of sample S2 and S9.

Table S2. Atomic parameters of sample S2 and S9 obtained from Rietveld refinement.

Sample	Atom	x/a	y/b	z/c	Occupancy
S2	Y	2/3	1/3	1/4	0.862
	Na1	2/3	1/3	1/4	0.138
	Na2	0	0	0.616(4)	0.06889
	O	0.3165(3)	0.4022(3)	1/4	0.483
	F	0.3165(3)	0.4022(3)	1/4	0.517
S9	Y	2/3	1/3	1/4	0.962
	Na1	2/3	1/3	1/4	0.038
	Na2	0	0	0.646(2)	0.019
	O	0.3142(3)	0.3918(4)	1/4	0.712
	F	0.3142(3)	0.3918(4)	1/4	0.288

Morphology.

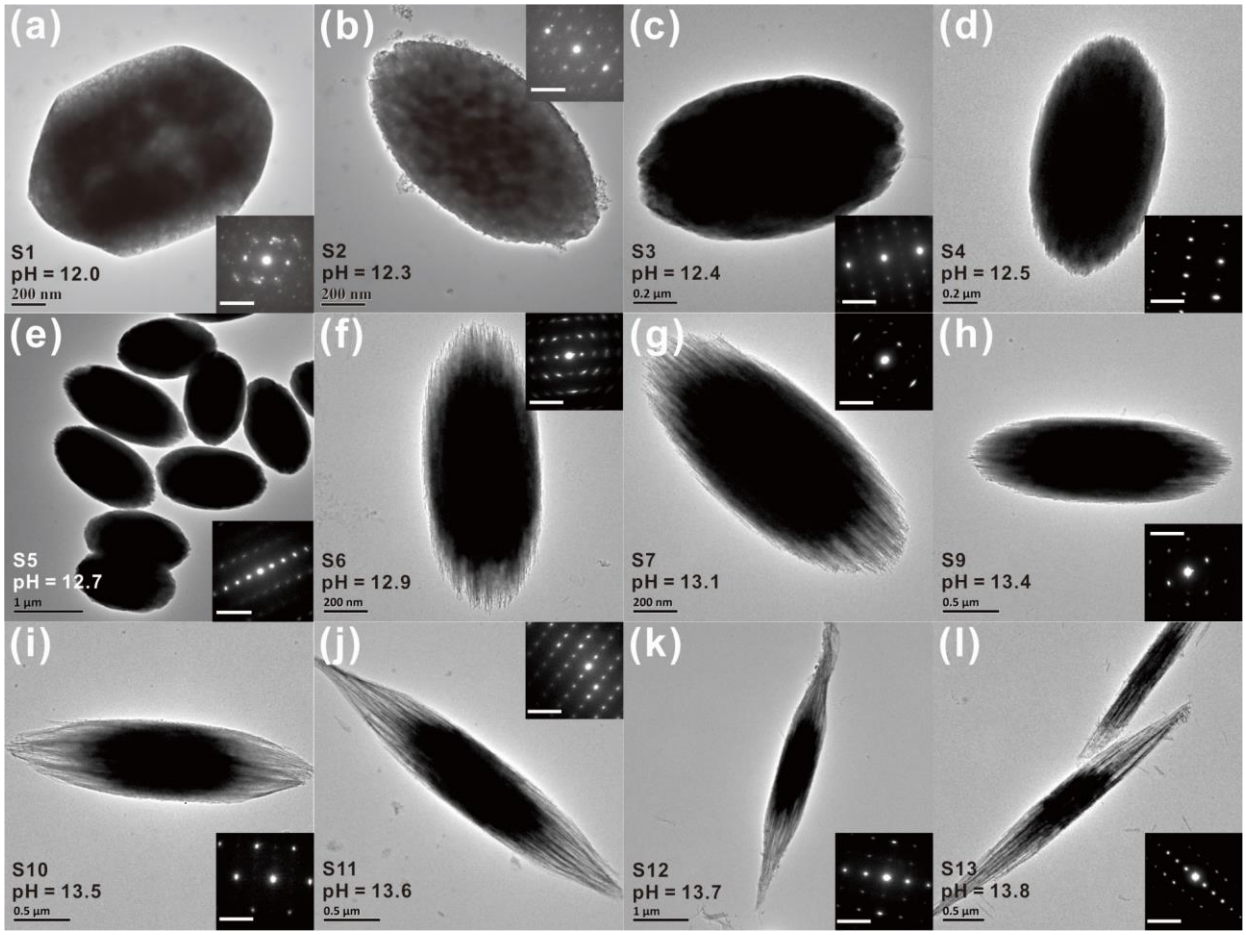

Figure S3. TEM images and SAED patterns (insets) of the as-prepared samples obtained in the initial solutions with different pH values. The scale bar in inset is 5 1/nm.

Luminescence Properties.

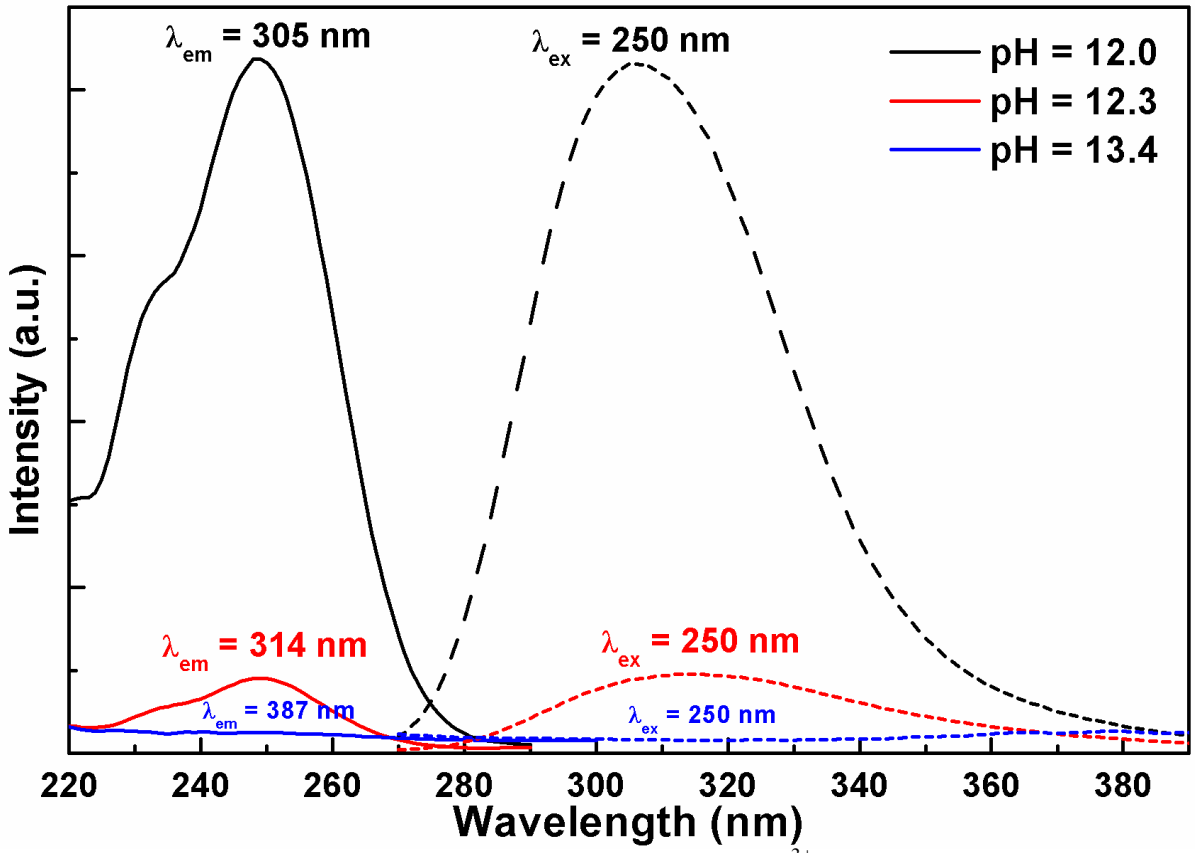

Figure S4. Excitation (left) and emission (right) spectra of Ce^{3+}-doped samples obtained under different pH values.

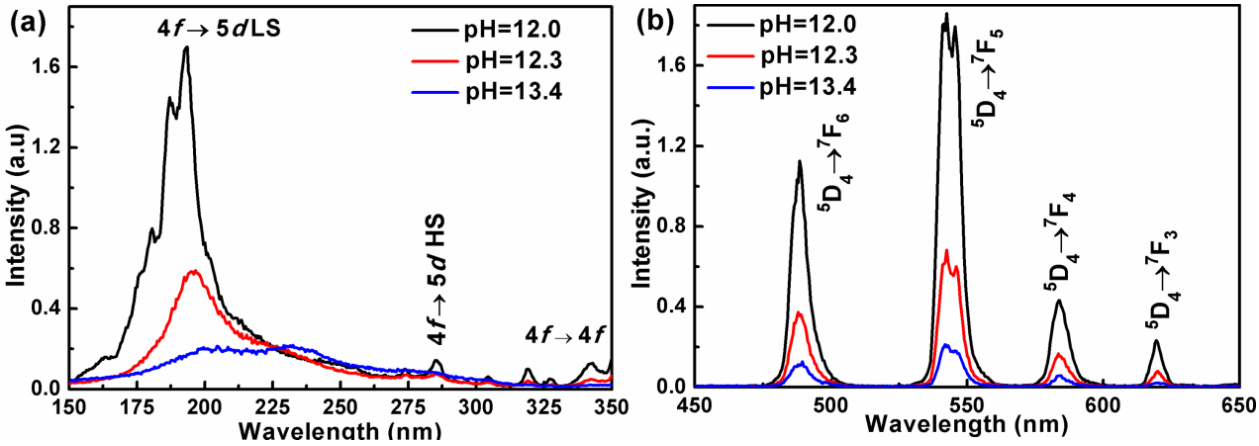

Figure S5. Excitation (a) and emission (b) spectra of Tb^{3+}-doped samples obtained under different pH values.

REFERENCES

(1) Rodríguez-Carvajal, J., Recent advances in magnetic structure determination by neutron powder diffraction. *Physica B* **1993,** 192, (1), 55-69.

(2) Nishizawa, H.; Okumoto, K.; Mitsushio, T., Preparation and thermal decomposition of yttrium hydroxide fluorides. *J. Solid State Chem.* **1991,** 92, (2), 370-379.

(3) He, X.; Yan, B., Yttrium hydroxide fluoride based monodisperse mesocrystals: additive-free synthesis, enhanced fluorescence properties, and potential applications in temperature sensing. *CrystEngComm* **2015,** 17, (3), 621-627.

(4) Christensen, A. N.; Hazell, R. G.; Ake, N., Hydrothermal Investigation of the Systems Y_2O_3-H_2O-Na_2O, Y_2O_3-D_2O-Na_2O, Y_2O_3-H_2O, and Y_2O_3-H_2O-NH_3. The Crystal Structure of $Y(OH)_3$. *Acta Chem. Scand.* **1967,** 21, 481-492.

(5) Mullica, D. F.; Milligan, W. O.; Beall, G. W., Crystal structures of $Pr(OH)_3$, $Eu(OH)_3$ and $Tm(OH)_3$. *J. Inorg. Nucl. Chem.* **1979,** 41, (4), 525-532.

(6) Beall, G. W.; Milligan, W. O.; Korp, J.; Bernal, I., The structure of terbium trihydroxide, $Tb(OH)_3$, by neutron diffraction. *Acta Crystallogr. Sect. B* **1977,** 33, (10), 3134-3136.